Case Studies in Thermal Engineering 45 (2023) 102946

Contents lists available at ScienceDirect

Case Studies in Thermal Engineering

journal homepage: www.elsevier.com/locate/csite

The novelty of using the AGM and FEM for solutions of partial differential and ordinary equations along a stretchable straight cylinder

As'ad Alizadeh [a], Fateme Sabet Sarvestani [b], Hussein Zekri [c,g], Mohsin O. AL-Khafaji [d,**], Hayder Mahmood Salman [e], Davood Domiri Ganji [f], Pooya Pasha [f,*]

[a] Department of Civil Engineering, College of Engineering, Cihan University-Erbil, Erbil, Iraq
[b] Department of Civil and Environmental Engineering, University of Houston, Texas, USA
[c] Department of Mechanical Engineering, College of Engineering, University of Zakho, Zakho, Iraq
[d] Air Conditioning and Refrigeration Techniques Engineering Department, Al-Mustaqbal University College, Babylon, 51001, Iraq
[e] Department of Computer Science, Al-Turath University College, Al Mansour, Baghdad, Iraq
[f] Department of Mechanical Engineering, Mazandaran University of Science and Technology, P.O. Box47166-85635, Babol, Iran
[g] College of Engineering, The American University of Kurdistan, Duhok, Kurdistan Region, Iraq

ARTICLE INFO

Keywords:
Suction/injection
Incompressible viscous flow
Finite element method
Stretching cylinder

ABSTRACT

Near the suction/injection area, a scientific definition for laminar boundary layer flow and heat transfer of an incompressible viscous flow over a stretching cylinder is given. In the study, differential equations with partial derivatives are converted into dimensionless coupled equations using numerical and analytical methods of **Akbari- Ganji and Finite Elements Methods**. The goal of this first stage of research and research on this topic is to use simplified forms to simplify equations using derivatives of simplified forms; the analysis of the displacement of the heat flux and the velocity gradient will be done using the changes of the Prandtl number. **Based on the results obtained on this issue,** it is found that the suction process increments surface firmness and quality, whereas the injection decreases surface skin friction. Also, at the points where the water and oil are attached to the surface of the cylinder, the heat has reached its maximum value, and as the distance increases along the Y axis, the temperature decreases. The highest temperature gradient is observed for water fluid. This shows that the use of water fluid around the cylinder accelerates the process of heat transfer from the surface to the outside of the boundary layer. One of the differences between the use of oil and water fluid around the cylinder according to the 2D contours is the difference in the temperature gradient of the two fluids. So that the highest temperature gradient is observed for water fluid.

1. Introduction

With technological advances, we are always looking for ways to deliver mechanical products more quickly and with superior quality. Science has an important role in achieving this goal. One of the most significant advances in science is in fluid mechanics. The

* Corresponding author.
** Corresponding author.
E-mail addresses: ghalama6@gmail.com (M.O. AL-Khafaji), Poooyaenginer@gmail.com (P. Pasha).

https://doi.org/10.1016/j.csite.2023.102946
Received 5 January 2023; Received in revised form 8 March 2023; Accepted 25 March 2023
Available online 29 March 2023

effect of fluid flow fields on stretching cylinders has attracted the attention of many researchers and has been comprehensively investigated. The combination of fluid mechanics science and mechanical issues has solved important engineering issues in industries [1–5]. Examining heat transfer and fluid flow on an expanding cylinder connected to hot rolling, refinery, and forming is vital for industries, and researchers are doing various studies to find better performance.

In the previous sentences, we discussed the definition of stretched cylinders and their applications in the engineering industry. A mathematical model can portray a system utilizing numerical concepts and language. The method of creating a mathematical model is named scientific modeling. Numerical models are used within the usual sciences (such as material science, science, soil science, and chemistry) and designing areas (such as computer science and electrical building), as well as in non-physical frameworks such as the social sciences (such as financial matters, brain research, human science, political science).

The utilization of scientific models to understand issues in commerce or military operations may be an expansive part of the field of

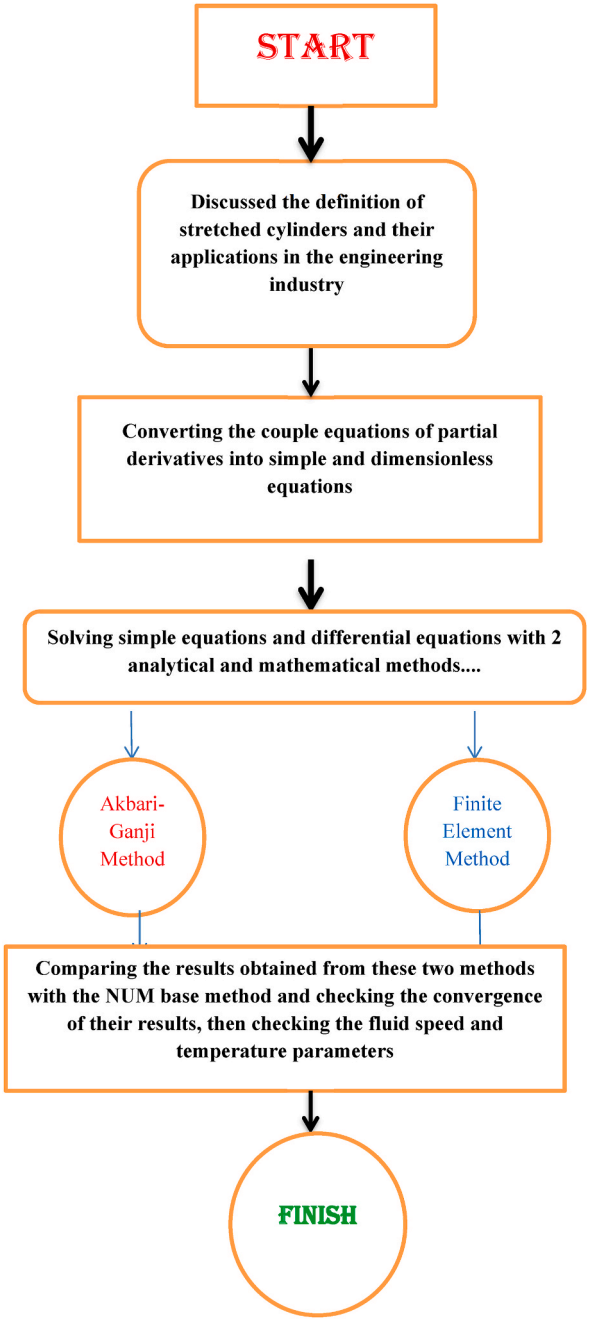

Fig. 1. aFlow chart of this quandary.

operations. Numerical models are utilized broadly in the music industry [6–10]. In science, a nonlinear framework could be a framework in which the alter of the results is not relative to the input change. Nonlinear issues intrigue engineers, biologists, physicists, mathematicians, and other researchers since most frameworks are undeniably nonlinear. Nonlinear dynamical frameworks, portraying changes in parameters over time, may appear weird, differentiating from much less complicated straight frameworks. A nonlinear equation is such that it does not frame a straight line. It looks like a bend in a chart. The significant contrast between linear and nonlinear conditions [11–15]. Another essential subject in mechanical engineering is the science of heat transfer. Heat exchange is the main factor for thermal designing that concerns the utilization, change, and transfer of heat vitality (warm) between physical frameworks.

Heat transfer is classified into three different types: conduction, convection, and radiation. Engineers moreover consider the mass exchange of contrasting chemical species (mass exchange within the frame of advection), either cold or hot, to realize heat exchange. Whereas these components have specific characteristics, they regularly happen at the same time within the same framework. Conduction is the coordination of small trades of active vitality of particles through the boundary between two frameworks. When a question is at a different temperature from another body or its environment, heat flows so that the body and the environment reach the same temperature. At this point, they are in heat equilibrium [16–20]. Another topic related to this article is the discussion of suction and injection. Suction/injection is utilized to control the liquid flow within the channel, and the exothermic chemical response of the Arrhenius dynamic is considered. Numerical results are displayed graphically and quantitatively to illustrate various parameters within the problem [21–31]. Toghraie and his colleagues [32–35] did a lot of research on entropy changes and heat transfer rates with mathematical and analytical methods. They analyzed them in various dimensions by using the finite element analysis methods and fluid numerical methods while solving differential coupled equations. The goal of this first stage of research and research on this topic is to use simplified forms to simplify equations using derivatives of simplified forms. the analysis of the displacement of the heat flux and the velocity gradient will be done using the changes of the Prandtl number.

In the second step, by using the finite element method, two fluids (water and oil) were added around the cylinder and investigated in various parameters to choose the most suitable fluid for this application. The novelty in this paper is the use of two analytical and mathematical engineering techniques, AGM and FEM. This transforms the equations from the differential to simple states and computes various fluid parameters such as the Prandtl and Nusselt numbers. In the framework of dimensionless equations. Among other innovations of this article, we can examine the differential equations with partial derivatives of this problem with the finite element method for the first time.

2. Mathematical modeling and governing equations

Near the suction/injection area, a scientific definition for laminar boundary layer flow and heat transfer of an incompressible viscous flow over an expandable-stretching horizontal cylinder (according to Fig. 1b) is given. The cylinder contracts/expands by changing its radius over time. Here the radius of the cylinder is granted to be a(t) = $a_0\sqrt{1-\beta t}$ in which a_0 is the radius of the cylinder at time t = 0 and β is a constant representing the contraction (β > 0) or expansion (β < 0) of the cylinder.

In the first part of the description of this research article, the dimensionless differential equations (Equations (8) and (9)) have been solved by Akbari Ganji's analytical and numerical method, and the changes in the fluid parameters of Prandtl number (Pr) and instability (A) are shown in 2D diagrams. In the second part, by using the primary equations of partial derivatives (equations (1)–(3)) and using the finite element method for their analysis, we obtained 3D contours of temperature changes and velocity changes around the pipe. **The mentioned texts are a summary of the objectives of this article.** Also, a flowchart is included in Figure 1a to guide the readers of this article.

In the lower part, energy and momentum equation forms are used for fluid flow [25]:

$$\frac{\partial}{\partial x}(ru^*)+\frac{\partial}{\partial r}(rw^*)=0, \tag{1}$$

$$\frac{\partial u^*}{\partial t}+u^*\frac{\partial u^*}{\partial x}+w^*\frac{\partial u^*}{\partial r}-\frac{\vartheta}{r}\frac{\partial}{\partial r}\left(r\frac{\partial u^*}{\partial r}\right)=0, \tag{2}$$

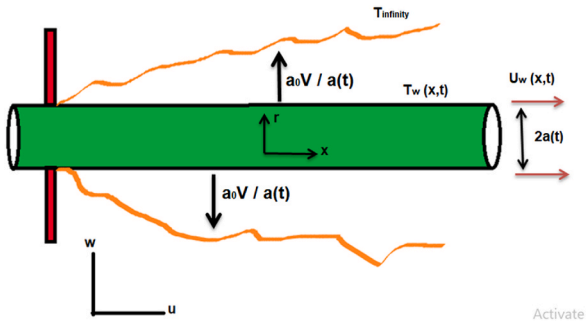

Fig. 1b. 2D image of the article schema.

$$\frac{\partial T^*}{\partial t}+u^*\frac{\partial T^*}{\partial x}+w^*\frac{\partial T^*}{\partial r}-\frac{a}{r}\frac{\partial}{\partial r}\left(r\frac{\partial T^*}{\partial r}\right)=0 \tag{3}$$

Depending on the boundary situations [25]:

$$r=a(t):u^*=U_w(x,t),w^*=\frac{a_0V}{a(t)},T^*=T_w^*(x,t), \tag{4}$$

$$\lim_{r\to\infty} u^*=0 \text{ and } \lim_{r\to\infty} T^*=T_\infty^* \tag{5}$$

Where (u^*) and (w^*) are the fluid velocity parts along x− and r − axes, respectively, ν is the fluid kinematic viscosity, T^* is the fluid temperature, α is the fluid thermal diffusivity and V is the suction (V < 0) or injection (V > 0) permanent.

The following equation is a dimensionless expression:

$$\eta=\frac{r^2}{a^2(t)}-1, \tag{6}$$

The above equation is utilized to turn the structure of partial differential conditions (1–3) into a simple differential condition framework. By using the dimensionless stress work, f(η), and the dimensionless temperature work, θ(η), the progression condition is fulfilled, and the momentum/energy equations are changed, resulting in:

$$u^*=\frac{U_w}{U_0}f'(\eta),w^*=\frac{-2\vartheta}{r}f(\eta),\theta(\eta)=\frac{T^*-T_\infty^*}{T_w^*-T_\infty^*}, \tag{7}$$

Equations (6) and (7) become simple non-linear equations by inserting and replacing them in equations (1)–(5) [26]:

$$(1+\eta)f'''+f''+ff''-(f')^2-A\{(1+\eta)f''+f'\}=0 \tag{8}$$

$$\frac{1}{Pr}\{(1+\eta)\theta''+\theta'\}+f\theta'-f'\theta-A\left\{(1+\eta).\theta'+\frac{1}{2}.\theta\right\}=0, \tag{9}$$

With the following boundary conditions [26]:

$$f(0)=-f0,f'(0)=U0,\theta(0)=1,\lim_{\eta\to\infty} f'(\eta)=0 \text{ and } \lim_{\eta\to\infty}\theta(\eta)=0, \tag{10}$$

Where primes signify separation with regard to η, $A=\beta a_0^2/4\vartheta$ is the instability parameter representing the strength of the cylinder contraction (A > 0) or expansion (A < 0), $Pr=\frac{\vartheta}{\alpha}$, is the Prandtl number, and $f_0=\frac{a_0}{2\nu}\nu$ is the suction or injection parameter.

The physical quantities of the cylindrical surface that we are interested in are the coefficient of surface friction, C_f, and the local Nusselt number, Nux, which are defined as:

$$C_f=2.\frac{\tau_w}{\rho U_w^2},NU_x=x.\frac{x.q_w}{k(T-T_\infty)}, \tag{11}$$

Where $\tau_w=\mu\left(\frac{\partial u^*}{\partial r}\right)_{r=R}$ is the cylinder´s shear stress, and $q_w=-k\left(\frac{\partial T^*}{\partial r}\right)_{r-R}$ is the cylinder´s sheet heat flux. By putting equations (6) and (7) in equation (11), the following expressions are obtained:

$$\frac{1}{2}.U_0C_f\sqrt{U_0Re_x}+f''(0)=0, and\ NU_x\sqrt{\frac{U_0}{Re_x}}+\theta'(0)=0 \tag{12}$$

According to the tables obtained from the AnsysFluent software (Tables 1a and 1b), the network of meshes and the number of networked elements around the cylinder with two fluids (water and oil) are displayed. The accuracy of meshing for both fluids is

Table 1A
Specifications of the network related to the mesh specification for oil.

Mesh specification for oil	
Method:	Patch Conforming, Tetrahedrons
Body Size Type:	Element Size
Size Function:	Curvature
Quality:	Medium
Medium Mesh:	Element Size: 0.5 mm
	Nodes: 3455
Fine Mesh:	Elements: 2987
	Nodes: 3778

defined in the same way, and only the number of elements for the oil is slightly more than that of water around the cylinder. For a better and more complete description of the meshes, two-dimensional graphs from grid independence test are given in Fig. 2. By looking at the graphs obtained for the temperature, it can be concluded that as the temperature changes more and more, the number of meshes on the cylinder and around the cylinder fluid increases and the quality of meshes become better.

3. Validation

The above 2D images reveal the convergence of thermal variables and fluid velocity around the stretched cylinder. According to the graphs depicted in Fig. 3, the beginning and the end of all the curves of the calculation methods are the same, which shows the convergence's correctness along the way. During calculating differential and simple equations, the convergence effect of the mentioned methods is significant so that a direct relationship can be found between the results of Akbari - Ganji and finite element methods with their convergence.

Table 1c illustrates a comparison between the results of fluid temperature changes around the cylinder between the present work and the studies of Fathy et al. [26]. Based on the values mentioned in the table at different distances from the cylinder surface for the temperature parameter, as the distance from the cylinder surface to the environment increases, the value of heat decreases, and this indicates that the highest temperature occurs around the thermal boundary layer of the extended cylinder surfaces.

4. Using the finite element method according to its advantages

The finite element method is one of the most important and widely used methods in solving linear and non-linear equations in various fluid and thermal engineering fields and mathematics. FEM is a popular numerical technique for dealing with half-multiplier difference conditions with two or three space factors (that is, some boundary estimation problems). For the vast majority of geometries and problems, Partial Differential Equations cannot be solved with analytical approaches. Instead, we can approximate these equations using discretization methods that can be solved using numerical methods. Therefore, the solutions we get are also an approximation of the real solution to those PDEs. The FEM is such an approximation method that subdivides a complex space or domain into a number of a small, countable and finite amount of pieces (thus the name finite elements) whose behavior can be described with comparatively simple equations. The basics of the method can be derived from Newton's laws of motion, conservation of mass and energy, and the laws of thermodynamics. At last, the finite element method definition of a boundary esteem issue comes about in a framework of logarithmic conditions. The premise of these strategies is to eliminate the differential equations or to simplify them to ordinary differential equations, which are solved by numerical methods such as Euler. Solving a partial differential equation is to arrive at a numerically stable simple equation. This means that the initial data and solution errors are insignificant, leading to incredible results. **There are methods with different advantages and disadvantages for this, of which the finite element method is one of the best.**

4.1. Using the Akbari-Ganji technique according to its advantages

Modeling nonlinear differential equation is more troublesome than understanding usual differential equations. In this respect, Akbari-Ganji's method (AGM) may be considered a practical arithmetical (semi-analytic) approach to understanding such issues. At first, an arrangement comprising obscure consistent coefficients is accepted within the AGM, fulfilling the differential condition and the initial conditions (IC). At that point, the unknown coefficients are computed utilizing logarithmic conditions obtained about IC and their subordinates. **One of the advantages of using this mathematical and analytical technique**. is that solving complicated and coupled equations with this method is much easier than with other methods. Due to its novelty, it has a high speed in solving equations and convergence of their results. Agreeing with the boundary condition, the typical model of a differential condition is as follows:

$$f(u^*, u^{*n}) = 0, n = 2, 3, \ldots \tag{13}$$

Differential condition is changed to arithmetical condition:

$$u^* = \sum_{k=0}^{m} a_k x^k \tag{14}$$

By substituting equ. (14) in to equ. (13), the taking after arrange is accessible:

Table 1b
Specifications of the network related to the mesh specification for water.

Mesh specification for water	
Method:	Patch Conforming, Tetrahedrons
Body Size Type:	Element Size
Size Function:	Curvature
Quality:	Medium
Medium Mesh:	Element Size: 0.5 mm
	Nodes: 3113
Fine Mesh:	Elements: 2239
	Nodes: 3030

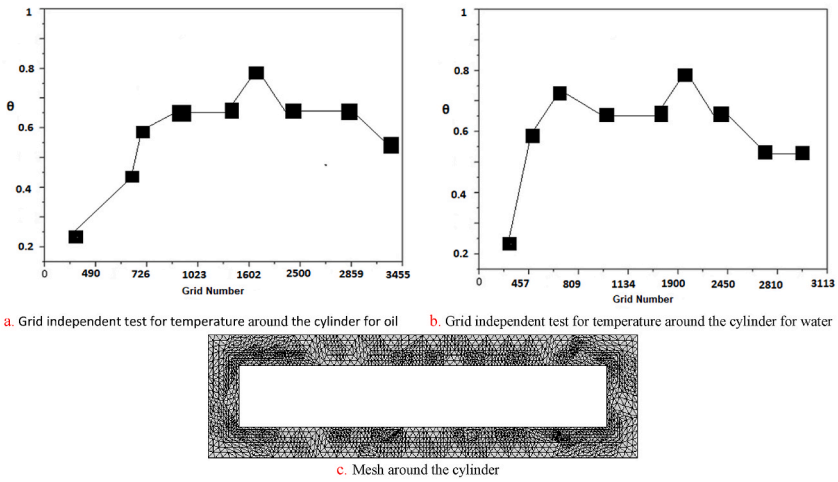

a. Grid independent test for temperature around the cylinder for oil b. Grid independent test for temperature around the cylinder for water

c. Mesh around the cylinder

Fig. 2. Grid independence test and Mesh geometry for stretched cylinder.

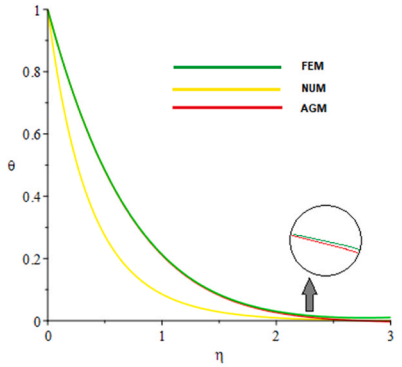

a. The graph of the temperature variable based on different distances on the cylinder with analytical methods.

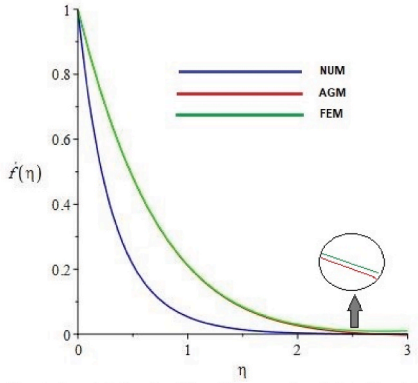

b. The graph of the velocity variable based on different distances on the cylinder with analytical methods.

Fig. 3. Convergence diagrams of results of finite element methods with AGM and Numeric.

Table 1c
Comparison of the solved results of this article (for temperature parameter) compared to the article of Dr. Fathy and his colleagues.

η	η = 0	η = 0.5	η = 1	η = 1.5	η = 2	η = 3	η = 4
Present work	1	0.37	0.09	0.05	0.02	0.01	0
Fathy et al. [26]	1	0.36	0.08	0.05	0.019	0.01	0

$$g(x)=f\left(\sum_{k=0}^{m}a_k x^k,\left\{\sum_{k=0}^{m}a_k x^k\right\}^{(n)}\right)=0 \tag{15}$$

By assuming n = 2 to condition (13), we have two boundary conditions within the underneath:

$$B.C: u^*(x)=u_0^* \quad at \gg x=0 \quad and \quad u^*(x)=u_l^* \quad at \gg x=L \tag{16}$$

Boundary conditions connected to condition (14) and (15) as takes after:

$$u^*(x)=\sum_{k=0}^{m}a_k x^k = a_0+a_1x^1+a_2x^2+\ldots..+a_m x^m \quad \leftrightarrow u^*(L)=u_1^*, u^*(0)=u_0^* \tag{17}$$

$$g(x=0)=0, g'(x=0)=0, g''(x=0)=0, \ldots\ g(x=L)=0, g'(x=L)=0, g''(x=L)=0, \ldots \tag{18}$$

5. Analysis of equations with the strategy of using methods

AGM's analytical and numerical solution method for the simplified and dimensionless equations of numbers 8 and 9 is investigated.

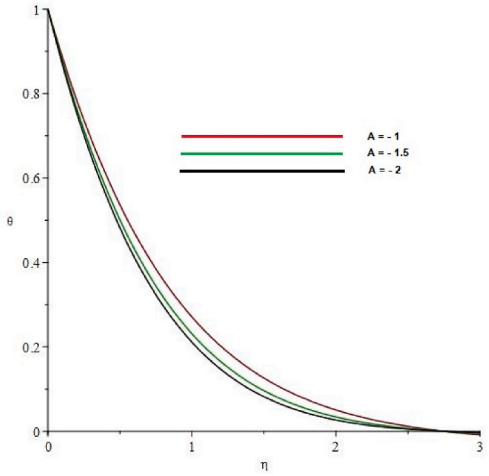

a. unsteadiness parameter for temperature unit

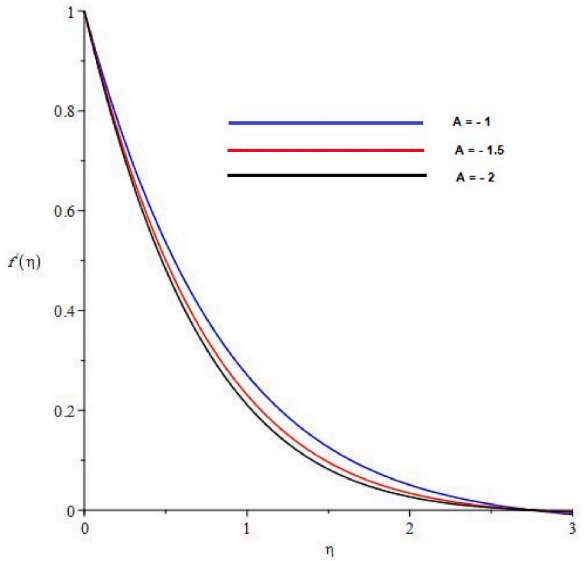

b. unsteadiness parameter for velocity unit

Fig. 4. Changes of the instability parameter in terms of the distance on the cylinder in relation to the fluid velocity and temperature.

$$f(\eta) = \sum_{i=0}^{5} a_i \eta^i = \eta^5 a_5 + \eta^4 a_4 + \eta^3 a_3 + \eta^2 a_2 + \eta a_1 + a_0 \tag{19}$$

$$\theta(\eta) = \sum_{i=0}^{5} b_i \eta^i = \eta^5 b_5 + \eta^4 b_4 + \eta^3 b_3 + \eta^2 b_2 + \eta b_1 + b_0 \tag{20}$$

Placement is performed by adding boundary conditions to the AGM conditions. The boundary conditions are:

$$a_0 = 1 \tag{21}$$

$$a_1 = 1 \tag{22}$$

$$a_1 + 5.50a_2 + 22.68a_3 + 83.18a_4 + 285.15a_5 = 0 \tag{23}$$

$$2.a_0.a_2 + 16.50.a_0.a_3 + 90.75.a_0.a_4 + 415.93.a_0.a_5 - 1.a_1^2 - 5.50.a_1.a_2 + 83.18.a_1.a_4 = 0 \tag{24}$$

$$6.a_0.a_3 + 66.a_0.a_4 + 453.7.a_0.a_5 - 2.a_1.a_2 + 90.75.a_1.a_4 + 831.87a_1a_5 - 11.a_2^2 = 0 \tag{25}$$

$$24.a_0.a_4 + 330.a_0.a_5 + 66.a_1.a_4 - 907.a_1.a_5 + 90.75.a_1.a_4 - 4.a_2^2 = 0 \tag{26}$$

$$b_0 = 1 \tag{27}$$

$$b_0 + 2.75.b_1 + 7.56.b_2 + 20.79.b_3 + 57.191.b_4 + 157.276.b_5 = 0 \tag{28}$$

$$a_0b_1 - 1.a_1b_0 + b_0 + 11.67b_1 + 67.38b_2 + 311.75b_3 + 1286.12b_4 + 4938b_5 = 0 \tag{29}$$

The solution is obtained by applying boundary conditions to the initial equation. Boundary conditions apply to the above equations. Regarding the above equations, we considered two test functions with eight constant coefficients and created nine equations. We can derive the equation as follows by substituting the coefficients obtained from the described actions under the following conditions:

$$f(\eta) = 0.001x^5 - 0.02.x^4 + 0.1.x^3 - 0.60.x^2 + 1.00x + 1 \tag{30}$$

$$\theta(\eta) = -0.002.\,x^5 + 0.03.\,x^4 - 0.23.\,x^3 + 0.7x^2 - 1.37x + 1 \tag{31}$$

6. Discussion-section

Here we discuss the effects of Prandtl number, suction/injection velocities on liquid velocity/temperature profiles, shear strain, and heat flow at the cylinder surface. The simulations carried out in this article are done by **Maple** and **AnsysFluent** engineering software. Numerical calculations of simplified and linear differential equations were done by Akbari Ganji methods, the usual numerical process in the Maple software environment, the meshing network around the cylinder, and the two-dimensional contours of Figs. 6 and 7 were done in the Ansys software environment. First, we analyze the one-dimensional graphs obtained from the AGM and NUM methods (Figs. 4 and 5). Fig. 4 shows an interpretation of the heat and heat transfer changes based on the instability parameter. As the estimate of the instability parameter A decreases, the radius of the cylinder increases. In Fig. (4 b), the frictional force between the liquid and the cylinder surface increases, it causes skin contact on the surface and slowing down the movement of the fluid. In the middle of the

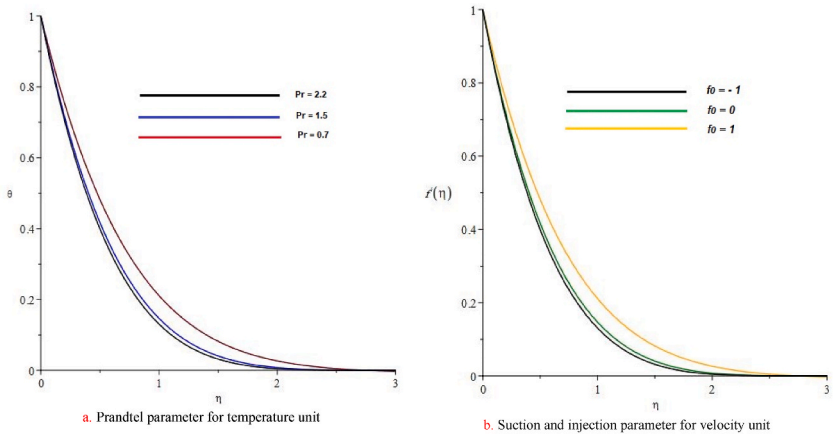

a. Prandtel parameter for temperature unit

b. Suction and injection parameter for velocity unit

Fig. 5. Changes of the Prandtel parameter and suction and injection parameter in terms of the distance on the cylinder in relation to the fluid velocity and temperature.

expansion of the cylinder radius, the area of the cylinder surface is enlarged, thereby increasing the rate of convective heat transfer. As the instability parameter A decreases and the instability values decrease, the heat flux of the fluid drops, and correspondingly, the Nusselt number decreases significantly (Fig. 4a). Picture 5-a shows the relationship between changes in the Prandtl number and the heat transfer rate of the fluid. Based on the observed findings, with the decrease of the Prandtl number, the temperature increases, and the heat transfer decreases. As the distance from the beginning of the cylinder surface to the outside of the boundary layer, the heat flux in different points of the cylinder surface includes the lowest value. The injection/suction parameter, f_0, can impact the heat transfer rate at the sheet by controlling the grinding between the liquid and the sheet. Suction permits the liquid streamlines to stay on the sheet more closely. This causes the frictional stress on the surface to increase, as shown in Fig. 5-b, the frictional strengths between the liquid layers increment, which decrease the fluid velocity.

When it comes to injection, the inverse behavior is seen. Now the interpretation of Fig. 6-a and 6-b is done using the finite element method. Fig. 6 is related to temperature changes for two studied fluids around the cylinder. As can be seen from the figures, at the points where the water and oil fluids are attached to the surface of the cylinder, the heat has reached its maximum value and as the distance increases along Y, the temperature decreases. In other words, with the growth of the thermal boundary layer and increase of the thickness of the boundary layer from the amount of heat transfer to the outside of the boundary layer decreases. Fig. 6-c and 6-d graphically depict temperature changes on the sides of the cylinder. One of the differences between the use of oil and water fluid around the cylinder according to the 2D contours is the difference in the temperature gradient of the two fluids. So that the highest temperature gradient is observed for water fluid. This shows that the use of water fluid around the cylinder accelerates the process of heat transfer from the surface to the outside of the boundary layer. Picture 7 examines the velocity gradient of oil and water around the cylinder. According to the results, the maximum velocity with an approximate value of 2.4 m/s has been obtained for water, which has lower viscosity than oil.

7. Conclusion (result section)

Examine the suction/injection area as one of the most important engineering problems because of their use in industries. In the study, differential equations with partial derivatives are converted into dimensionless coupled equations using numerical and analytical methods of **Akbari- Ganji and finite** element **methods**. **The purpose of the study** is to simplify the equations with derivatives in a simplified form so that by using the simplified form, the analysis of the changes in the heat flux and the velocity gradient will be done by using the Prandtl number. In the second step, using the finite element method, the water, and oil were added around the cylinder and then compared together to choose the most suitable fluid. **Based on the results obtained on this issue,** it is found that the suction process increments surface firmness and quality, whereas the injection diminishes surface skin friction. In addition, at the points where the water and oil fluids are attached to the surface of the cylinder, the heat has reached its maximum value. As the distance increases along the Y axis, the temperature decreases. The highest temperature gradient is observed for water fluid. This interpretation shows that the use of water fluid around the cylinder accelerates the process of heat transfer from the surface to the outside of the boundary layer.

- The accuracy of meshing for both fluids is defined in the same way, and only the number of elements and networks formed for the oil fluid is slightly more than that of water around the cylinder.
- One of the advantages of using the AGM mathematical and analytical technique is that solving heavy and coupled equations with this method is much easier than other methods. Due to its novelty, it has a high speed in solving equations and convergence of their results.
- One of the differences between the use of oil and water fluid around the cylinder according to the 2D contours is the difference in the temperature gradient of the two fluids. So that the highest temperature gradient is observed for water fluid.

Authorship statement

Category 1.

Conception and design of study: As'ad Alizadeh: Department of Civil engineering, College of engineering, Cihan University-Erbil, Erbil, Iraq.

Acquisition of data: Pooya Pasha: Department of mechanical Engineering Mazandaran University of science and technology, P.O. Box47166-85635, Babol, Iran.

Analysis and/or interpretation of data: Hayder Mahmood Salman and Davood Domiri Ganji: Department of Computer Science, Al-Turath University College, Al Mansour, Baghdad, Iraq.

Department of mechanical Engineering Mazandaran University of science and technology, P.O. Box47166-85635, Babol, Iran.

Category 2.

Drafting the manuscript: Fateme Sabet Sarvestani: Department of Civil and Environmental Engineering, University of Houston, Texas, US.

Revising the manuscript critically for important intellectual content: Mohsin O. AL-Khafaji and Hussein Zekri: Air conditioning and Refrigeration Techniques Engineering Department, Al-Mustaqbal University College, Babylon 51,001, Iraq.

Department of mechanical engineering, College of engineering, University of Zakho, Zakho, Kurdistan Region-Iraq.

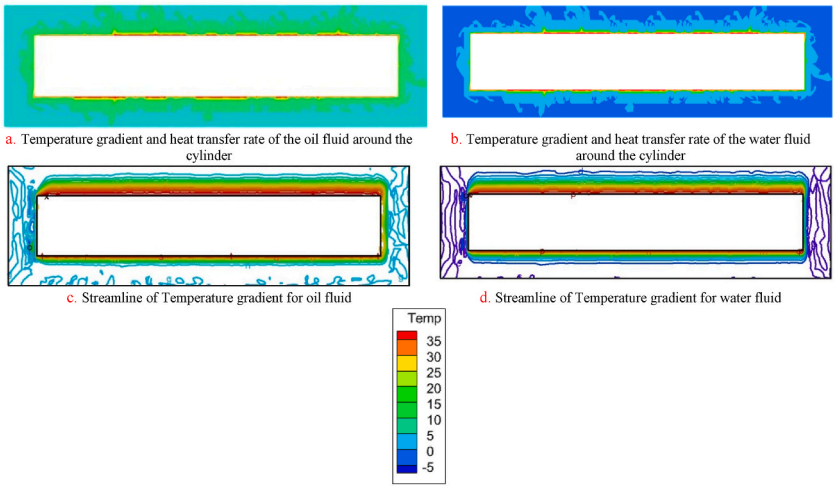

Fig. 6. Diagrams of thermal changes of oil and water fluids around the cylinder.

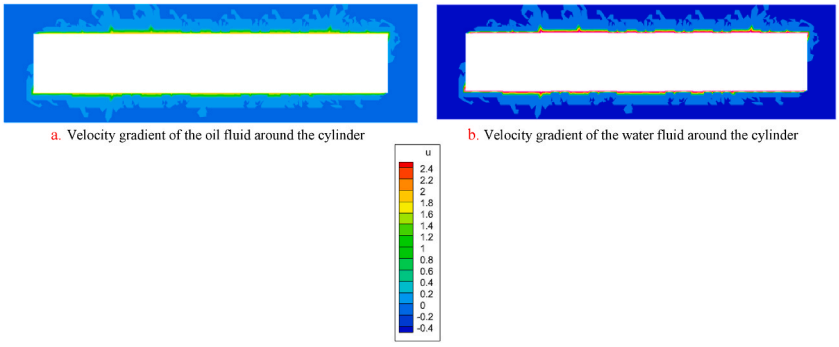

Fig. 7. Diagrams of velocity changes of oil and water fluids around the cylinder.

Declaration of competing interest

The authors declare that they have no known competing financial interests or personal relationships that could have appeared to influence the work reported in this paper.

Data availability

Data will be made available on request.

Nomenclature

U,v,w = velocity component
Pr = Prandtel number
k = Thermal conductivityT = = Thermal conductivityT = Temperature
t = Time
T_w^* = fluid temperature
α = fluid thermal diffusivity
A = instability parameter
f_0 = suction or injection parameter
C_f = coefficient of surface friction
Nu = Nusselt number
τ_w = Cylinder is shear stress
q_w = cylinder sheet warm flux

References

[1] Aisha M. Alqahtani, et al., Thermal analysis of a radiative nanofluid over a stretching/shrinking cylinder with viscous dissipation, Chem. Phys. Lett. 808 (2022), 140133.
[2] Y. Dharmendar Reddy, et al., Heat absorption/generation effect on MHD heat transfer fluid flow along a stretching cylinder with a porous medium, Alex. Eng. J. 64 (2022) 659–666.
[3] Ali Qasemian, et al., Hydraulic and thermal analysis of automatic transmission fluid in the presence of nano-particles and twisted tape: an experimental and numerical study, J. Cent. S. Univ. 28 (11) (2021) 3404–3417.
[4] Muhammad Yasir, et al., Mathematical modelling of unsteady Oldroyd-B fluid flow due to stretchable cylindrical surface with energy transport, Ain Shams Eng. J. 14 (2023) 1, 101825.
[5] Reza Iranmanesh, et al., Introducing a linear empirical correlation for predicting the mass heat capacity of biomaterials, Molecules 27 (19) (2022) 6540.
[6] Pooya Pasha, Saeid Mirzaei, Meysam Zarinfar, Application of numerical methods in micropolar fluid flow and heat transfer in permeable plates, Alex. Eng. J. 61 (4) (2022) 2663–2672.
[7] Reza Fathollahi, et al., Applying numerical and computational methods to investigate the changes in the fluid parameters of the fluid passing over fins of different shapes with the finite element method, International Journal of Thermofluids 15 (2022), 100187.
[8] Paria Shadman, et al., Combined septum and chamfer fins on threated stretching surface under the influence of nanofluid and the magnetic parameters for rotary seals in computer hardware, Alex. Eng. J. 62 (2023) 489–507.
[9] Marzieh Karimzadeh, et al., Heat transmission and magnetic effects on a ferrofluid liquid in a hybrid survey under the influence of two Helmholtz coils, Results in Engineering 16 (2022), 100702.
[10] Mohammad Nabizadeh, Abhinendra Singh, Safa Jamali, Structure and dynamics of force clusters and networks in shear thickening suspensions, Phys. Rev. Lett. 129 (2022) 6, 068001.
[11] Ferdosi, Sima Besharat, Maryam Abasi, Axial buckling of single-walled nanotubes simulated by an atomistic finite element model under different temperatures and boundary conditions, Int. J. Sci. Eng. Appl. 11 (11) (2022) 151–163.
[12] M. Mudassar Gulzar, et al., A nonlinear mathematical analysis for magneto-hyperbolic-tangent liquid featuring simultaneous aspects of magnetic field, heat source and thermal stratification, Appl. Nanosci. 10 (12) (2020) 4513–4518.
[13] M. Zubair, et al., A theoretical study on partial slip impact in radiative-hydromagnetic liquid configured by extending surface, Int. J. Mod. Phys. B (2022), 2350074.
[14] M.S. Sadeghi, et al., Analysis of thermal behavior of magnetic buoyancy-driven flow in ferrofluid–filled wavy enclosure furnished with two circular cylinders, Int. Commun. Heat Mass Tran. 120 (2021), 104951.
[15] M. Waqas, et al., Effect of nonlinear convection on stratified flow of third grade fluid with revised Fourier-Fick relations, Commun. Theor. Phys. 70 (1) (2018) 25.
[16] N. Sandeep, Ram Prakash Sharma, M. Ferdows, Enhanced heat transfer in unsteady Magnetohydrodynamic nanofluid flow embedded with aluminum alloy nanoparticles, J. Mol. Liq. 234 (2017) 437–443.
[17] Sharma, Ram Prakash, S.R. Mishra, A numerical simulation for the control of radiative heat energy and thermophoretic effects on MHD micropolar fluid with heat source, J. Ocean Eng. Sci. 7 (1) (2022) 92–98.
[18] M.M. Khader, Ram Prakash Sharma, Evaluating the unsteady MHD micropolar fluid flow past stretching/shirking sheet with heat source and thermal radiation: implementing fourth order predictor–corrector FDM, Math. Comput. Simulat. 181 (2021) 333–350.
[19] Pooya Pasha, et al., Hybrid investigation of thermal conductivity and viscosity changeable with generation/absorption heat source, Comput. Therm. Sci.: Int. J. 14 (2022) 1.
[20] Abdollahzadeh, Mohammad Javad, et al., Surveying the hybrid of radiation and magnetic parameters on Maxwell liquid with TiO2 nanotube influence of different blades, Heat Transfer 51 (6) (2022) 4858–4881.
[21] Pooya Pasha, et al., Examination of warm transfer on extending sheet by variation iteration method strategy and investigation of arrangements for optimizing liquid properties, Engineering Reports 4 (2022) 10, e12505.
[22] Reza Fatehinasab, et al., Hybrid surveying of radiation and magnetic impacts on Maxwell fluid with MWCNT nanotube influence of two wire loops, ZAMM-Journal of Applied Mathematics and Mechanics/Zeitschrift für Angewandte Mathematik und Mechanik 103 (2023) 1, e202200186.
[23] Reza Fathollahi, et al., Analyzing the effect of radiation on the unsteady 2D MHD Al2O3-water flow through parallel squeezing sheets by AGM and HPM, Alex. Eng. J. 69 (2022) 207–219.
[24] S.A. Abdollahi, et al., Computer simulation of Cu: ALOOH/Water in a microchannel heat sink using a porous media technique and solved by numerical analysis AGM and FEM, Theoretical and Applied Mechanics Letters (2023), 100432.
[25] E.M.A. Elbashbeshy, T.G. Emam, M.S. El-Azab, K.M. Abdelgaber, Slip effect on flow, heat, and mass transfer of a Nanofluid over a stretching horizontal cylinder in the presence of suction/injection, Therm. Sci. 20 (6) (2016) 1813–1824.
[26] Mohamed Fathy, K.M. Abdelgaber, Semi-analytical solutions of flow and heat transfer of fluid along expandable-stretching horizontal cylinder, Case Stud. Therm. Eng. 28 (2021), 101426.
[27] P. Pasha, et al., Chemical reaction-diffusion model around a vessel for studying temperature and concentration of three chemical species by finite element method, Int. J. Eng. 36 (1) (2023) 171–181.
[28] P. Pasha, D. Domiri-Ganji, Hybrid analysis of micropolar ethylene-glycol nanofluid on stretching surface mounted triangular, rectangular and chamfer fins by FEM strategy and optimization with RSM method, Int. J. Eng. 35 (5) (2022) 845–854.
[29] A.I.S.S.A. Abderrahmane, et al., Non-Newtonian nanofluid natural convective heat transfer in an inclined Half-annulus porous enclosure using FEM, Alex. Eng. J. 61 (7) (2022) 5441–5453.
[30] Hossein Nabi, Mohsen Pourfallah, Mosayeb Gholinia, Omid Jahanian, Increasing heat transfer in flat plate solar collectors using various forms of turbulence-inducing elements and CNTs-CuO hybrid nanofluids, Case Stud. Therm. Eng. ISSN: 2214-157X 33 (2022), 101909, https://doi.org/10.1016/j.csite.2022.101909.
[31] H. Nabi, M. Gholinia, D.D. Ganji, Employing the (SWCNTs-MWCNTs)/H2O nanofluid and topology structures on the microchannel heatsink for energy storage: a thermal case study, Case Stud. Therm. Eng. ISSN: 2214-157X 42 (2023), 102697, https://doi.org/10.1016/j.csite.2023.102697.
[32] Weal Al-Kouz, et al., Heat transfer and entropy generation analysis of water-Fe3O4/CNT hybrid magnetic nanofluid flow in a trapezoidal wavy enclosure containing porous media with the Galerkin finite element method, The European Physical Journal Plus 136 (11) (2021) 1184.
[33] Hejazi, Seyed Amir Mousavian, et al., Numerical investigation of rigidity and flexibility parameters effect on superstructure foundation behavior using three-dimensional finite element method, Case Stud. Constr. Mater. (2023), e01867.
[34] Aiien Moarrefzadeh, et al., Fabrication and finite element simulation of 3D printed poly L-lactic acid scaffolds coated with alginate/carbon nanotubes for bone engineering applications, Int. J. Biol. Macromol. 224 (2022) 1496–1508.
[35] H. Liang, et al., Investigation of the effect of Berkovich and Cube Corner indentations on the mechanical behavior of fused silica using molecular dynamics and finite element simulation, Ceram. Int. 48 (19) (2022) 28781–28789.